Journal of Zhejiang University-SCIENCE C (Computers & Electronics)
ISSN 1869-1951 (Print); ISSN 1869-196X (Online)
www.zju.edu.cn/jzus; www.springerlink.com
E-mail: jzus@zju.edu.cn

Design considerations for electromagnetic couplers in contactless power transmission systems for deep-sea applications*

Ze-song LI†, De-jun LI†, Lin LIN, Ying CHEN†‡

(*State Key Lab of Fluid Power Transmission and Control, Zhejiang University, Hangzhou 310027, China*)

†E-mail: zesonlee@gmail.com; li_dejun@zju.edu.cn; ychen@zju.edu.cn

Received Nov. 17, 2009; Revision accepted June 2, 2010; Crosschecked Sept. 3, 2010

Abstract: In underwater applications of contactless power transmission (CLPT) systems, high pressure and noncoaxial operations will change the parameters of electromagnetic (EM) couplers. As a result, the system will divert from its optimum performance. Using a reluctance modeling method, we investigated the gap effects on the EM coupler in deep-sea environment. Calculations and measurements were performed to analyze the influence of high pressure and noncoaxial alignments on the coupler. It was shown that it is useful to set a relatively large gap between cores to reduce the influence of pressure. Experiments were carried out to verify the transferring capacity of the designed coupler and system for a fixed frequency. The results showed that an EM coupler with a large gap can serve a stable and efficient power transmission for the CLPT system. The designed system can transfer more than 400 W electrical power with a 2-mm gap in the EM coupler, and the efficiency was up to 90% coaxially and 87% non-coaxially in 40 MPa salt water. Finally, a mechanical layout of a 400 W EM coupler for the underwater application in 4000-m deep sea was proposed.

Key words: Contactless power transmission (CLPT), EM coupler, Deep sea, Gap effects
doi:10.1631/jzus.C0910711 **Document code:** A **CLC number:** TM131.4+1

1 Introduction

In ocean exploration, underwater vehicles are always powered by secondary batteries. However, battery charging in underwater environments is always difficult due to the conductivity and high pressure of sea water. Traditional conducting approaches have intrinsic faults in these applications, such as the risk of electric shock and contact wear. The contactless power transmission (CLPT) system has overwhelming advantages because of its high sealing quality to surrounding sea water (Kojiya *et al.*, 2004; 2005). In this system, an electromagnetic (EM) coupler is used as a transferring interface between the vehicle and the underwater station. The EM coupler is divided into two separated parts, the primary and secondary sides. The primary side is mounted on the station as the energy transmitter. The secondary side is mounted on the vehicle as the receiver. A vehicle comes to the cable station before the battery energy is used up, fixing its secondary side to the primary side to get the battery recharged. Consequently, energy can be transmitted via the EM link between the two sides without any electrical connection to the source, avoiding dangerous electric shock in sea water and strict friction.

CLPT systems have been investigated for decades and widely utilized in many fields such as power transmission for electric vehicles (Covic *et al.*, 2007; Villa *et al.*, 2009), implantable electronics in biomedical devices (Si *et al.*, 2008; Jung *et al.*, 2009), and portable devices (Choi *et al.*, 2004; Liu and Hui, 2008). In these applications, the EM coupler's properties were intensively studied, and air-gap effects on power losses have been analyzed (Papastergiou and

‡ Corresponding author

* Project supported by the National High-Tech R & D Program (863) of China (No. 2007AA091201), the Natural Science Foundation of Zhejiang Province, China (No. Y5090117), and the Qianjiang Excellence Project of Zhejiang Province, China (No. 2009R10036)

Macpherson, 2007a; 2008). Different structures of cores and windings were compared to obtain optimized parameters and capacities (Ayano *et al.*, 2004; Liu and Hui, 2008). In recent years, this approach has been introduced into ocean engineering (Feezor *et al.*, 2001; McGinnis *et al.*, 2007; Yoshioka *et al.*, 2007). However, in deep-sea applications, the coupler's properties largely depend on the surrounding environment.

In the deep sea, high pressure is one of the main factors affecting the EM coupler, causing a reduction in the magnetic permeability of ferrite cores (Loaec *et al.*, 1978; le Floch *et al.*, 1981). As a result, inductances of the coupler will decrease in the deep-sea environments (Zhang *et al.*, 2008). Another problem is the awkward operation of an EM coupler, the two sides of which are difficult to align coaxially in underwater environments. Moreover, random turbulence can change the alignment. Noncoaxial alignments result in further changes in inductance. Accordingly, the noncoaxial tolerance should be improved to ensure the power transmission.

The inductances of a coupler are strongly related with its geometry and its material property, especially the gap between cores. Because sea water in the gap is nonferromagnetic, the influence on inductances varies greatly. Therefore, in order to keep inductances insensitive to high-pressure sea water and improve the noncoaxial tolerance, the gap between cores should be specially selected.

This study aims at resolving these problems, providing an efficient and stable EM coupler for CLPT systems to be used in the deep sea. Based on the analysis of the physical structure and magnetic coupling, the equivalent electric circuit was presented to investigate the characteristics of the EM coupler. Considering the high pressure and noncoaxial alignment in sea water, the magnetizing inductance was calculated by means of reluctance modeling. Based on the analysis, an EM coupler with P48 pot cores and a 2-mm gap was designed. Furthermore, parameters were measured by an LCR meter to verify the calculations. The results showed that a relatively large gap will reduce the sensitivity of the EM coupler to high pressure. Several experiments were carried out to test the coupler in salt water at 40 MPa. Experiments showed that the CLPT system with the designed coupler can transfer more than 400 W electrical power to the load with high efficiency, up to 90% coaxially and 87% noncoaxially in high pressure salt water. Finally, a mechanical implementation was proposed.

2 Analysis of the contactless power transmission system

Fig. 1a illustrates the application of an EM coupler in charging an underwater vehicle. Fig. 1b shows how the CLPT system works, presenting the circuit structures of primary and secondary sides of the coupler. The primary circuit converts the supplied DC voltage into high-frequency square AC voltage, provided to the primary winding of the EM coupler. Correspondingly, the secondary side serves its inducted voltage to the load after rectification. It is the mutual inductance M that links the two side circuits via magnetic coupling, transferring electric energy by a contactless approach. Considering the actual operating situation shown in Fig. 1a, the EM coupler is designed to be axially symmetric (Fig. 1c), so that the angle orientation in alignment can be eliminated and more easily matched.

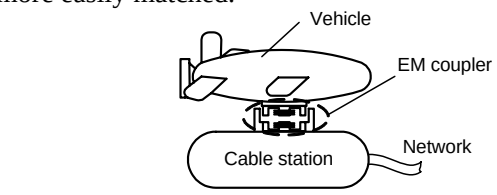

(a)

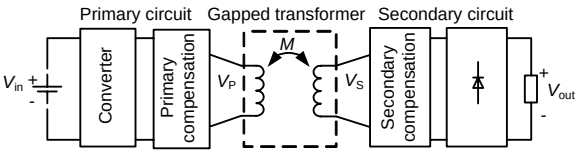

(b)

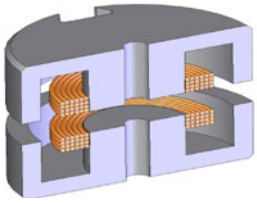

(c)

Fig. 1 Illustration of the contactless power transmission (CLPT) system used in underwater applications
(a) Application of a CLPT system; (b) Schematic diagram of the system; (c) Physical structure of the electromagnetic (EM) coupler

Due to the physical separation, the EM coupler exhibits a low coupling coefficient k, low magnetizing inductance and high leakage inductance (Fernandez *et al.*, 2002; Papastergiou and Macpherson, 2007a). The equivalent circuit model for the EM coupler is as shown in Fig. 2. This model illustrates the coupler as an ideal transformer combined with a magnetizing circuit.

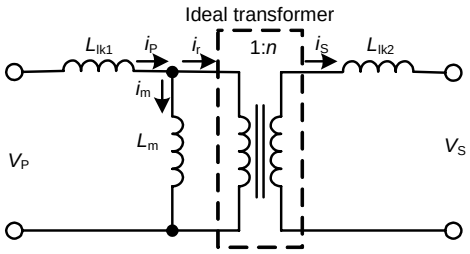

Fig. 2 Equivalent circuit of the electromagnetic coupler

Magnetizing inductance L_m and leakage inductances L_{lk1} and L_{lk2}, can be described by self-inductances L_P and L_S and mutual inductance M, which can be measured directly by an LCR meter. The relationship among them is given by Eqs. (1)–(3) as follows (Hayes *et al.*, 2003; Ryu *et al.*, 2005):

$$L_m = Mn, \tag{1}$$

$$L_{lk1} = L_P - Mn = L_P(1-k), \tag{2}$$

$$L_{lk2} = L_S - M/n = L_S(1-k), \tag{3}$$

where n is the turns ratio of the ideal transformer, and k is the coupling coefficient between primary and secondary windings, which is given by

$$k = M/\sqrt{L_P L_S}. \tag{4}$$

Low coupling means low transferring power and efficiency of the system. To deal with this problem, compensation is necessary in order for the CLPT system to improve its transferring ability (Fig. 1b). Several kinds of compensations have been investigated, suggesting different characters for various applications (Stielau and Covic, 2000; Wang *et al.*, 2004). In this study, the compensation with a series capacitance in the primary side and a parallel capacitance in the secondary side (SP topology) was selected (Fig. 3a). In this circuit, the output AC voltage of the EM coupler with compensation is rectified and filtered to DC voltage and provided to the loading resistance. To make it clear, the loading condition of the EM coupler is simplified to the equivalent impedance Z_L that acts approximately as a resistive load, which is $Z_L=8R_L/\pi^2$. And then the equivalent circuit of the system (Fig. 3b) can be derived. As a result, the resonant frequency of the circuit is given by

$$f_r = \frac{1}{2\pi\sqrt{L_S C_S}} = \frac{1}{2\pi\sqrt{L_P C_P(1-k^2)}}, \tag{5}$$

where C_P and C_S are the compensated capacitances in each side of the coupler. In order to maximize the transferring capacity and efficiency, the fixed switching frequency of the converter is set equal to the resonant frequency f_r. Obviously, if the self-inductances L_P and L_S are changed during working, the system will divert from its optimum situation, resulting in dropped transferring capacity. Unfortunately, this is almost unavoidable in deep-sea applications, due to high-pressure seawater and noncoaxial operations. In this work we investigate the gap effects on the parameters to design a less susceptible structure of the EM coupler in underwater environments.

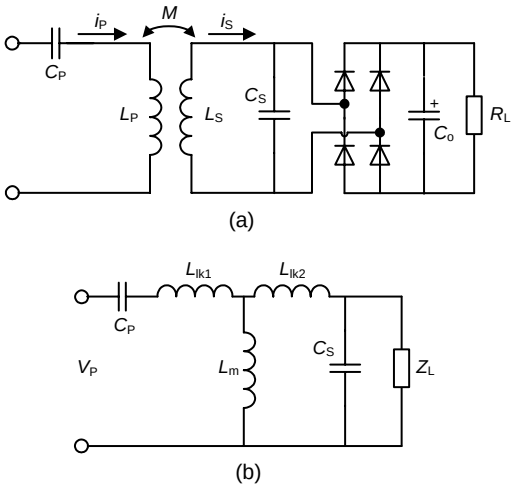

Fig. 3 The contactless power transmission (CLPT) circuit model with SP (series-parallel) compensation
(a) Topology of the CLPT system; (b) Equivalent circuit of the system

3 Gap effects on the electromagnetic coupler

To investigate the behaviors of the EM coupler in the deep sea, the reluctance modeling method was used. This method presents magnetic circuits with reluctances in the coupler's structure (Wang *et al.*, 1999). As a result, corresponding inductances can be calculated. Therefore, this method can be used to explore gap effects on reducing the influence of high pressure and misalignment.

3.1 Reluctance modeling

The flux paths in the coaxially aligned coupler are shown in Fig. 4a, including the main flux and leakage flux paths. Fig. 4a also suggests that the effect of the flux passing through each path can be modeled by assigning a proper reluctance (the equivalent of resistance in an electric network) whose value is related with the material permeability, the cross-sectional area, and the length of the path. Consequently, the equivalent magnetic circuit can be obtained as shown in Fig. 4c. Fig. 4b illustrates the paths of a noncoaxially aligned coupler. On the basis of some reasonable assumptions (Hirai *et al.*, 2000), the reluctance R_j of path j can be calculated as

$$R_j = \frac{l_j}{\mu_{rj}\mu_0 A_j}, \tag{6}$$

where l_j is the length, A_j is the cross-sectional area, μ_{rj} is the relative permeability of the magnetic path j, and $\mu_0=4\pi\times10^{-7}$ H/m is the magnetic permeability of vacuum.

This circuit can be divided into three sub-circuits, α, β, and γ. The flux of sub-circuit α traverses through both primary and secondary windings, so it corresponds to the magnetizing inductance in the equivalent circuit as shown in Fig. 4d. Thus, the magnetizing inductance can be calculated as

$$\begin{aligned} L_{\mathrm{m}} &= N_{\mathrm{P}}^2 \big/ (R_{\mathrm{m\_c1}} + R_{\mathrm{m\_c2}} + R_{\mathrm{m\_g1}} + R_{\mathrm{m\_g2}}) \\ &= N_{\mathrm{P}}^2 \mu_0 A_{\mathrm{e}} \big/ (l_{\mathrm{c}} / \mu_{\mathrm{rc}} + l_{\mathrm{g}}), \end{aligned} \tag{7}$$

where N_{P} is the number of the primary windings, A_{e} is the effective cross-sectional area of the path, l_{c} is the effective length of flux path in cores, μ_{rc} is the relative permeability of ferrite cores, and l_{g} is the effective length of the gap.

Similarly, the leakage inductances corresponding to sub-circuits β and γ can be presented as

$$L_{\mathrm{lk1}} = N_{\mathrm{P}}^2 \big/ (R_{\mathrm{m\_c1}} + R_{\mathrm{m\_lk1}}) = N_{\mathrm{P}}^2 \mu_0 A_{\mathrm{lk1}} \big/ (l_{\mathrm{c}} / \mu_{\mathrm{rc}} + l_{\mathrm{lk1}}), \tag{8}$$

$$L_{\mathrm{lk2}} = N_{\mathrm{S}}^2 \big/ (R_{\mathrm{m\_c2}} + R_{\mathrm{m\_lk2}}) = N_{\mathrm{S}}^2 \mu_0 A_{\mathrm{lk2}} \big/ (l_{\mathrm{c}} / \mu_{\mathrm{rc}} + l_{\mathrm{lk2}}), \tag{9}$$

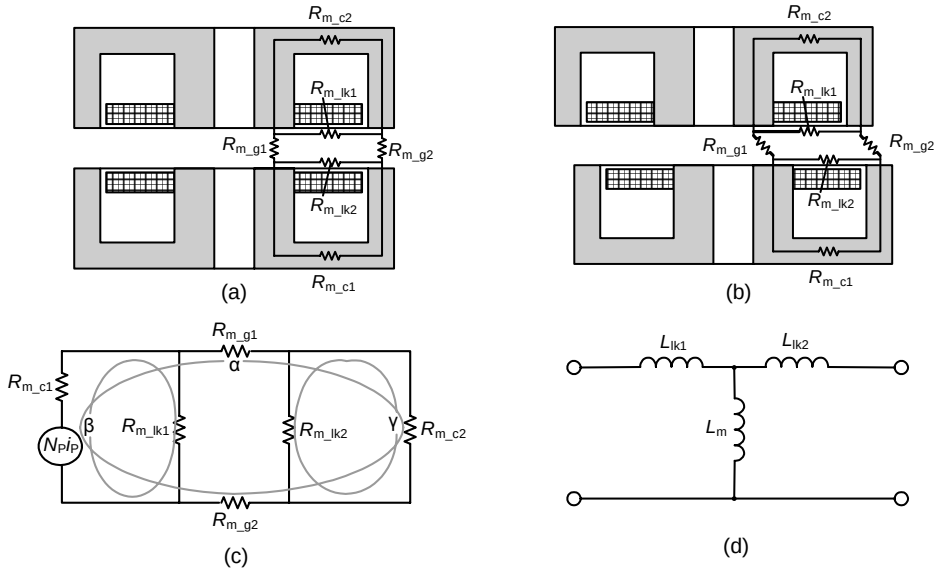

Fig. 4 Reluctance model of the electromagnetic coupler with pot cores

(a) Flux paths of the coupler with coaxial alignment; (b) Flux paths of the coupler with noncoaxial alignment; (c) Equivalent magnetic circuit for the electromagnetic coupler; (d) Equivalent electrical circuit for the electromagnetic coupler

where N_S is the number of turns of secondary winding, l_{lk1} and l_{lk2} are the effective lengths, and A_{lk1} and A_{lk2} are the equivalent cross-sectional areas of the leakage flux paths in primary and secondary sides, respectively. For the high (over 2000) permeability of ferrite cores, it should be noted that $l_c/\mu_{rc} << l_{lk}$, so the leakage inductance is determined mainly by l_{lk1} and l_{lk2}.

3.2 High-pressure influence

The high pressure of seawater is the most important property in the deep-sea environment, leading to a reduction in the magnetic permeability of ferrite cores because of the material's piezomagnetic property. The relationship between initial permeability and pressure can be described by the following equation (Loaec *et al.*, 1975):

$$\frac{\mu_{rc}(P)}{\mu_{rc}(0)} = \frac{1}{1 + c\mu_{rc}(P) \cdot P}, \tag{10}$$

where $\mu_{rc}(0)$ and $\mu_{rc}(P)$ refer to the relative permeability of the ferrite core in atmosphere and at pressure P, respectively, and c is a constant of the ferrite material. As the pressure increases from atmospheric pressure to 40 MPa, the permeability of ferrite materials will be reduced by more than 40% (le Floch *et al.*, 1981).

As deduced from Eqs. (6)–(9), only the magnetizing inductance is influenced largely by the reduced permeability in high-pressure seawater. To maintain a constant magnetizing inductance, the total reluctance of sub-circuit α should be immune to the permeability of cores. Therefore, the effective permeability is used to represent the average permeability in the magnetic circuit, which is defined as

$$\mu_e = \mu_0 \frac{l_c + l_g}{l_c / \mu_{rc} + l_g}. \tag{11}$$

Eq. (11) suggests that the effective permeability is dependent on the ratio of the effective length of cores, l_c/μ_{rc}, and the length of the gap, l_g. If $l_c/\mu_{rc} << l_g$, the magnetizing inductance will have little susceptibility to the high pressure.

In this work, P48 type pot cores of TDK PC40 ferrite were selected, their relative permeability being about 2300. The experimental EM coupler with this kind of core had 25-turn Lizt wire winding in each side. Experiments showed that when the core is exposed to sea water with a pressure up to 40 MPa, its relative permeability is reduced to about 1400 (Loaec *et al.*, 1978). According to Eq. (7), the magnetizing inductance L_m will decrease and the reluctance will increase correspondingly (Fig. 5a). On the other hand, a large gap provides a large reluctance to the sub-circuit α, which is immune to high pressure. Furthermore, gap reluctances become dominant in magnetizing reluctance R_{m_α}, and the effective permeability μ_e is determined mainly by gap length l_g. As a result, the magnetizing inductance will be little affected by high pressure.

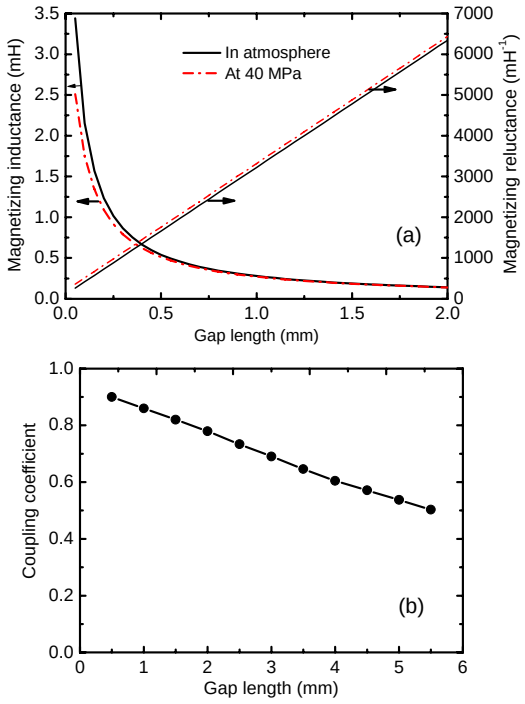

Fig. 5 Gap effects on the electromagnetic (EM) coupler
(a) Magnetizing inductances and magnetic reluctances of the EM coupler in atmosphere and 40-MPa-pressure water; (b) Coupling efficient as a function of gap length

Additionally, it is clear that the variation of the magnetizing inductance is less at a large gap than at a small one (Fig. 5a). This is important for system modeling to obtain stable parameters and good resonant conditions. To quantify this variation, the variable D is used, which is expressed as

$$D = -\frac{1}{L_{\mathrm{m}}}\frac{\mathrm{d}L_{\mathrm{m}}}{\mathrm{d}l_{\mathrm{g}}} \times 100\%. \quad (12)$$

This indicates the rate of change of the inductance per millimeter when the gap varies. Values of the three parameters at different gaps are compared in Table 1. It is obvious that an EM coupler can achieve much more stable inductances when the gap is 2 mm, because D is only 48% (the gap always changes within a half millimeter).

However, the increased gap affects not only the pressure sensitivity and the variation of inductances, but also the coefficient of the EM coupler, which is very important in power transferring. As shown in Fig. 5b, the coefficient is reduced with the gap length increasing. A low coefficient seriously limits the transferring power and efficiency of the CLPT system. Although compensation is used, the coefficient should be guaranteed at some high level. In this investigation, at least 0.5 is needed. Considering the applying conditions, such as the core type and the sea depth, the gap length is therefore selected as 2 mm. As shown in Figs. 5a and 5b, the magnetizing inductance decreases by only 1.5% at a high pressure of 40 MPa, and the coefficient of the EM coupler is about 0.76, which is high enough.

Table 1 Parameters of the coupler at three different gaps

Parameter	Value		
	0.1 mm	0.5 mm	2.0 mm
Magneting reluctance, R_{m_α} ($\mu\mathrm{H}^{-1}$)	417.5	1664.5	6340.9
Magnetizing inductance, L_{m} (μH)	1.75	0.50	0.13
Changing rate of the inductance, D (%)	608	177	48

To measure the parameters, the EM coupler was enclosed in a high-pressure test chamber filled with salt water, and the pressure was adjusted from atmospheric pressure to 40 MPa. As a result, the primary self-inductance is normalized as shown in Fig. 6a, and the coupling coefficients are shown in Fig. 6b. Comparing the two parameters of the same

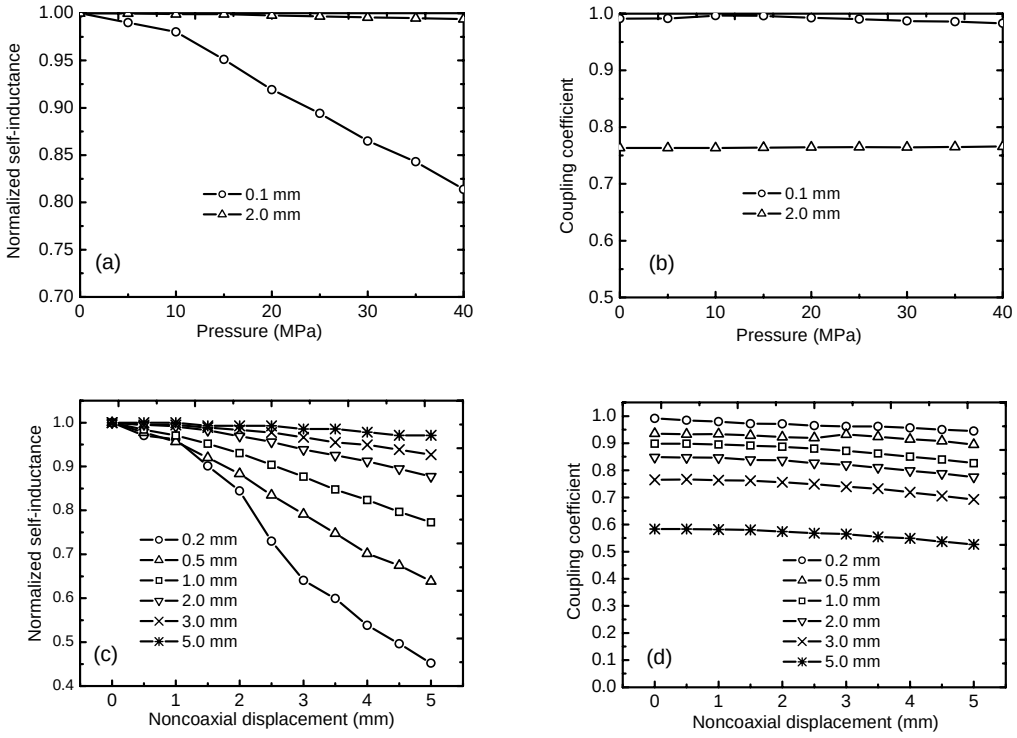

Fig. 6 Gap effects on the electromagnetic coupler

(a) Normalized primary self-inductances of the coupler under different pressures and with 0.1 mm and 2 mm gap lengths, respectively; (b) Coupling coefficients of the coupler under different pressures and with 0.1 mm and 2 mm gap lengths, respectively; (c) Normalized primary self-inductances of the coupler with different gap lengths and noncoaxial displacements; (d) Coupling coefficients of the coupler with different gap lengths and noncoaxial displacements

coupler with 0.1 mm and 2 mm gaps, it is clear that the large gap has good effect on reducing the pressure influence.

3.3 Noncoaxial tolerance

Misalignment is almost unavoidable in underwater CLPT systems, so that a high misalignment tolerance is required to ensure the transferring capability. The misaligned coupler is shown in Fig. 4b with equivalent reluctances in the flux paths. It is obvious that the equivalent gap length is larger than that in coaxial alignment, resulting in larger reluctance and more leakage flux of the coupler. According to Eq. (7), the magnetizing inductance and the coupling coefficient are both decreased.

Fig. 6c shows that the self-inductance with a relatively large gap is less changeable than that with a small gap. When the gap length is only 0.2 mm, the self-inductance will be reduced by about 55% as the noncoaxial displacement X increases from 0 mm to 5 mm. However, it is only about 12% and 7% when the gap length is 2 mm and 3 mm, respectively. Nevertheless, when X increases in the same range, the reductions of coupling coefficients with different gap lengths are similar within about 5% (Fig. 6d). This means that a relatively large gap makes the inductance more robust against misalignment as well as against high pressure. Furthermore, the 2-mm gap selected in solving the pressure effect is also appropriate to misalignments.

4 Experimental verification

Based on aforementioned analysis, we designed an EM coupler with P48 ferrite cores and 25-turn winding in both primary and secondary sides (Fig. 7a). The adopted gap length between cores was 2 mm, while the coaxially-aligned and 5-mm-misaligned couplers are shown in Fig. 7b. Inductances and coupling coefficients were measured when couplers were enclosed in the chamber filled with 40-MPa-pressure salt water and these are presented in Table 2. Fig. 8 shows the experimental facilities. The wire of the coupler was sealed by a plastic tube filled with oil, and connected with the outside circuits by a pair of waterproof connecters. These facilities isolated the circuits from conductive salt water.

(a)

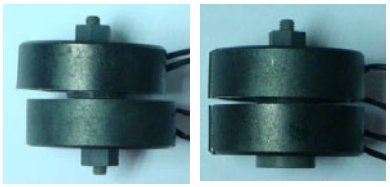

(b)

Fig. 7 The 2-mm-gap electromagnetic coupler with P48 pot cores and Litz wire windings

(a) Core halves with windings; (b) Coaxial and noncoaxial alignments of the coupler

Table 2 The coupler's parameters in experiments

Parameter	Value	
	e=0 mm	e=5 mm
Primary inductance, L_P (μH)	130.0	118.2
Secondary inductance, L_S (μH)	129.4	117.2
Mutual inductance, M (μH)	99.0	82.4
Coupling coefficient, k	0.765	0.701

Fig. 8 High-pressure chamber and experimental facilities

The electric circuits of a CLPT system include the primary converter and secondary rectifier (Fig. 9). In these circuits, the secondary compensated capacitance C_S is 22 nF and the primary one C_P is 50 nF. According to Eq. (5) and the parameters shown in Table 2, the resonant frequency is 94.3 kHz for coaxial alignment.

Consequently, the switching frequency of the converter is set to 94.3 kHz to obtain the maximum transferring capacity. The converter is fabricated by using the IRFP250N power MOSFET, providing more than 400 W to the primary winding with a

supplied 110 V voltage. In this circuit, the parasitic components of the coupler and the switches were used to achieve zero voltage switching (ZVS) by the phase shift full bridge (PSFB) topology (Papastergiou and Macpherson, 2007b). This topology contributes immensely to the efficient power transferring, since the ZVS can reduce the power losses of switches during the switching periods. The fabricated PSFB converter is shown in Fig. 10.

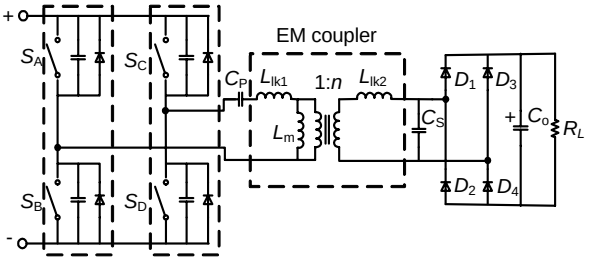

Fig. 9 The phase shift full bridge (PSFB) topology of the contactless power transmission (CLPT) system with a primary converter and a secondary rectifier-filter

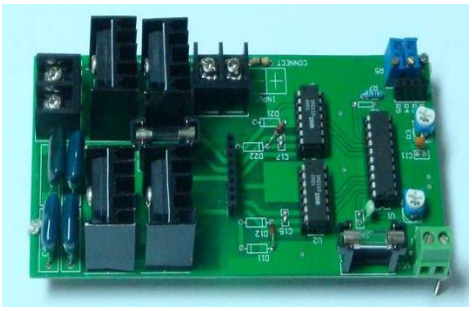

Fig. 10 The fabricated converter of the contactless power transmission (CLPT) system

During the experiments, the four MOSFET switches were controlled by drain voltages from the controller and they converted the supplied DC voltage to a high-frequency AC voltage. As shown in Fig. 11a, waveforms of the drain voltages were set to make the converter obtain PSFB. Fig. 11b illustrates waveforms of the output voltage of the converter (V_P) and the current in the secondary winding (i_S) of the coupler. It is clear that the current was transformed to an approximate sine-wave by means of the resonant compensation, in spite of the square-wave supplied voltage by the converter. This is important for a CLPT system that the capability and efficiency can be improved greatly (Green and Boys, 1994).

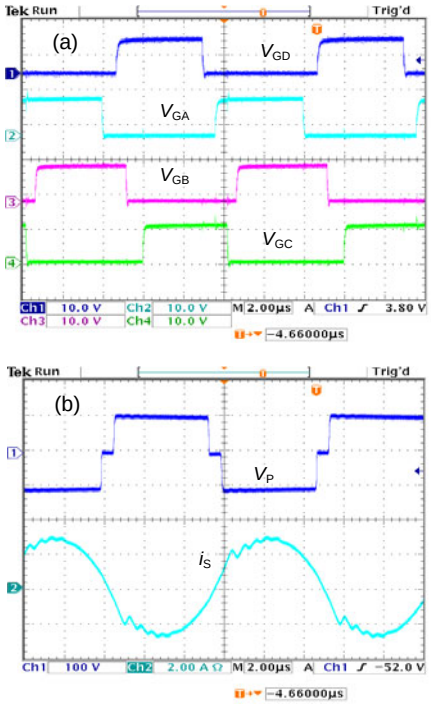

Fig. 11 Typical waveforms of the working contactless power transmission (CLPT) system

(a) The waveforms of the driving voltage for the four MOSFET switches; (b) The waveforms of the converter's output voltage V_P and the secondary current of the coupler i_S

The EM coupler has been tested under a series of different environments, including in air and in salt water (at atmospheric pressure and 40 MPa, respectively). The experimental results are shown in Fig. 12, describing the transferring ability of the CLPT system with an EM coupler. In Fig. 12a, the output voltages are represented as functions of the load current, as well as the output powers shown in Fig. 12b and efficiencies shown in Fig. 12c.

The results suggest that power transferring in atmospheric salt-water differs little from that in air. As the pressure increases to 40 MPa (representing 4000-m deep sea), the efficiency decreases a little. This is due to the increased magnetizing current in the primary windings, because the magnetizing inductance is compressed by the high pressure. Owing to the gap between cores, however, the efficiency decreases by only 1%–2%, which is accessible. On the other hand, the misalignment affects the transmission much more significantly. The output voltage of the secondary circuit drops by about 5 V from that of the

coaxial coupler. Nevertheless, this system has a regulated output power and high efficiency greater than 85%, when the loading current is up to 1.5 A. In actual performance, it is easy to keep the noncoaxial displacement within 5 mm, as mentioned in the following section; thus, the CLPT system can transfer power at a high level in practical applications.

In summary, a 2-mm gap between the cores can effectively diminish the pressure influence on the EM coupler and maintain regulation output against misalignments of the EM coupler. The system is capable of transferring more than 400 W power to the load in deep sea, being comparable to those ashore systems.

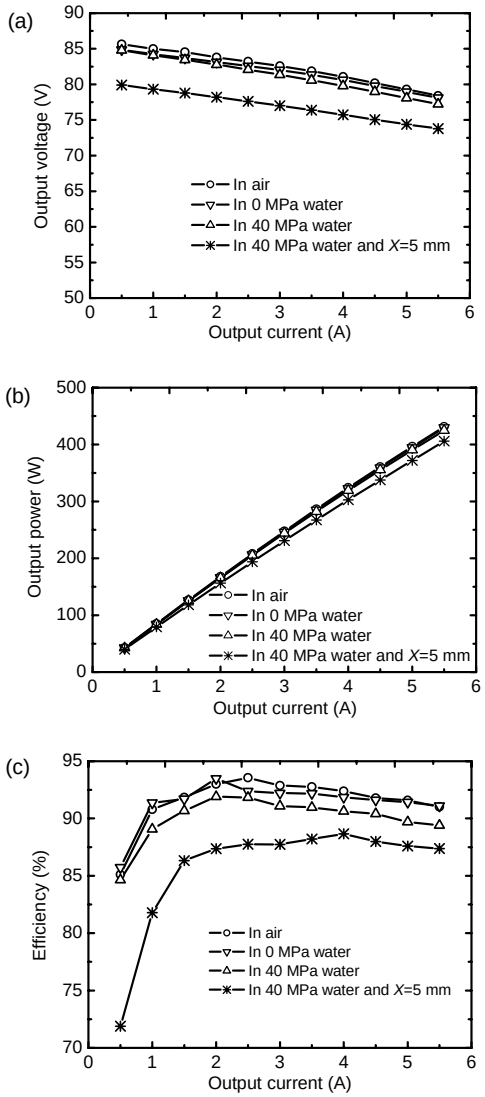

Fig. 12 Experimental results of the power transferring
(a) Output voltages to the load with corresponding load currents; (b) Output powers to the load with corresponding load currents; (c) Transferring efficiency of the contactless power transmission (CLPT) system

5 Mechanical implementation

When designing the EM coupler housing, there are several requirements related to the following:

1. The chemical property of the housing material should be steady to avoid corrosion by salt water in long-term applications.

2. The two sides should be easily mated without complex locating equipments.

3. The mated coupler should be robust against random turbulences in the deep-sea environment.

4. Electromagnetic interference (EMI) of the coupler should be taken into account.

An initially designed housing for the EM coupler appears in Fig. 13.

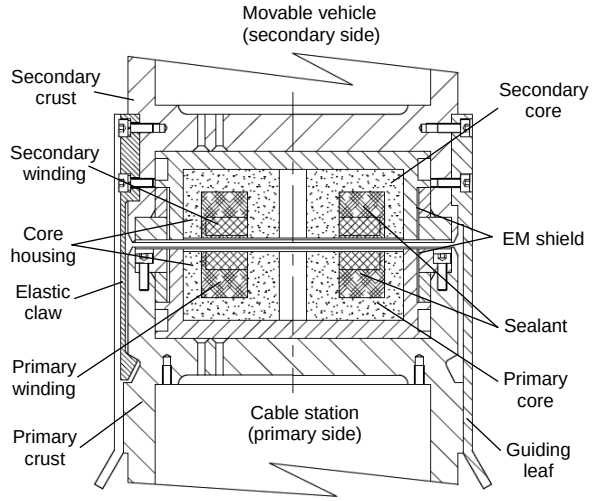

Fig. 13 Assembly of the electromagnetic coupler
The top part has elastic claws and guiding leaves, this being the secondary side of the structure; the bottom part has a wedge-shaped groove outside, this being the primary side. The thickness of the housing is 5 mm, which can bear high pressure in 4000-m deep sea

The structure (Fig. 13) meets all the above requirements for the package of the EM coupler. The primary and secondary crusts are made of titanium alloy TC4, which has a very steady electro-chemical property for avoiding corrosion in sea water. The core housings in both sides are made of nylon, which is ductile enough to protect the brittle ferrite cores from

sudden collisions. Afterwards, the two sides of the EM coupler can be operated easily with the guiding leaves, and fixed by claws. Consequently, the mated coupler is stable enough against random turbulences. In addition, a thin copper sheet is added around the core housing as the EM shield. Taking account of the skin effect, the thickness of the sheet should be smaller than the skin depth δ_0, depending on the operating frequency f_w:

$$\delta_0 = \sqrt{1/(\pi f_w \mu_0 \sigma)}, \quad (13)$$

where σ=5.882×10^7 S/m is the electrical conductivity of copper. Thus, the shield is set to be 0.05 mm thick to avoid a large eddy current.

During operations, the secondary crust will become coaxial with the primary one via the guiding leaves. Thus, it is easily located before the two sides mate. The claws on the secondary crust can be pushed open in radius direction by the primary crust until its triangular head is inserted into the groove. The two windings are therefore coupled with each other for power transmission. The front angle of the claw is much larger than the rear one. This is for the sake of easy mating and a fixed axial position of the EM coupler during the power transmission. The gap between cores fluctuates within a small range of 0.3 mm, so that the magnetic interface is guaranteed. Meanwhile, the radial movement is limited by the guiding leaves. Thus, the EM coupler has a benign coupling condition after mating.

6 Conclusions

In this paper, we investigated an EM coupler with relatively large gap and for use in deep-sea applications. The coupler can transfer electrical energy from cable stations to mobile vehicles via magnetic coupling. Considering the actual deep-sea environment, we analyzed the influence of the high pressure and misalignment of cores on the EM coupler, describing the magnetizing inductance and leakage inductance by a series of calculations. Using the reluctance modeling method and measurements, the gap effects on the EM coupler were analyzed.

Depending on the analysis, an EM coupler with P48 pot cores having a 2-mm gap was designed for the CLPT system, transferring the required several hundred watts electrical powers to the load. Experiments were carried out to test the ability of the system in high-pressure salt water. The results showed that the system can transfer more than 400 W electrical power with about 90% efficiency, and that the coupler with a 2-mm gap exhibited a high degree of stability in high-pressure water and under a misaligned condition. The housing for the EM coupler was designed, with a mechanical structure suitable to be applied in a 4000-m deep sea.

References

Ayano, H., Nagase, H., Inaba, H., 2004. A highly efficient contactless electrical energy transmission system. *Electr. Eng. Jpn.*, **148**(1):66-74. [doi:10.1002/eej.10290]

Choi, B., Nho, J., Cha, H.Y., Ahn, T., Choi, S., 2004. Design and implementation of low-profile contactless battery charger using planar printed circuit board windings as energy transfer device. *IEEE Trans. Ind. Electron.*, **51**(1):140-147. [doi:10.1109/TIE.2003.822039]

Covic, G.A., Boys, J.T., Kissin, M.L.G., Lu, H.G., 2007. A three-phase inductive power transfer system for roadway-powered vehicles. *IEEE Trans. Ind. Electron.*, **54**(6):3370-3378. [doi:10.1109/TIE.2007.904025]

Feezor, M.D., Sorrell, F.Y., Blankinship, P.R., Bellingham, J.G., 2001. An interface system for autonomous undersea vehicles. *IEEE J. Ocean. Eng.*, **26**(4):522-525. [doi:10.1109/48.972087]

Fernandez, C., Garcia, O., Prieto, R., Cobos, J.A., Uceda, J., 2002. Overview of Different Alternatives for the Contactless Transmission of Energy. Proc. 28th Annual Conf. of the IEEE Industrial Electronics Society, **1-4**:1318-1323. [doi:10.1109/IECON.2002.1185466]

Green, A.W., Boys, J.T., 1994. 10 kHz Inductively Coupled Power Transfer: Concept and Control. Proc. 5th Int. Conf. on Power Electronics and Variable-Speed Drives, **399**:694-699. [doi:10.1049/cp:19941049]

Hayes, J.G., O'Donovan, N., Egan, M.G., O'Donnell, T., 2003. Inductance Characterization of High-Leakage Transformers. 18th Annual IEEE Applied Power Electronics Conf. and Exposition, **1-2**:1150-1156. [doi:10.1109/APEC.2003.1179361]

Hirai, J., Kim, T.W., Kawamura, A., 2000. Study on intelligent battery charging using inductive transmission of power and information. *IEEE Trans. Power Electron.*, **15**(2):335-345. [doi:10.1109/63.838106]

Jung, K.H., Kim, Y.H., Kim, J., Kim, Y.J., 2009. Wireless power transmission for implantable devices using inductive component of closed magnetic circuit. *Electron. Lett.*, **45**(1):21-22. [doi:10.1049/el:20092241]

Kojiya, T., Sato, F., Matsuki, H., Sato, T., 2004. Automatic Power Supply System to Underwater Vehicles Utilizing Non-contacting Technology. MTS/IEEE Techno-Ocean, **1-4**:2341-2345. [doi:10.1109/OCEANS.2004.1406521]

Kojiya, T., Sato, F., Matsuki, H., Sato, T., 2005. Construction of Non-contacting Power Feeding System to Underwater Vehicle Utilizing Electro Magnetic Induction. Europe Oceans, **1-2**:709-712. [doi:10.1109/OCEANSE.2005.1511801]

le Floch, M., Loaec, J., Pascard, H., Globus, A., 1981. Effect of pressure on soft magnetic-materials. *IEEE Trans. Magn.*, **17**(6):3129-3134. [doi:10.1109/TMAG.1981.1061600]

Liu, X., Hui, S.Y.R., 2008. Optimal design of a hybrid winding structure for planar contactless battery charging platform. *IEEE Trans. Power Electron.*, **23**(1):455-463. [doi:10.1109/TPEL.2007.911844]

Loaec, J., Globus, A., le Floch, M., Johannin, P., 1975. Effect of hydrostatic pressure on magnetization mechanisms in Ni-Zn ferrite. *IEEE Trans. Magn.*, **11**(5):1320-1322. [doi:10.1109/TMAG.1975.1058884]

Loaec, J., le Floch, M., Johannin, P., 1978. Effect of hydrostatic-pressure on susceptibility frequency spectrum of polycrystalline Mn-Zn and Ni-Zn ferrites. *IEEE Trans. Magn.*, **14**(5):915-917. [doi:10.1109/TMAG.1978.1059 959]

McGinnis, T., Henze, C.P., Conroy, K., 2007. Inductive Power System for Autonomous Underwater Vehicles. OCEANS, **1-5**:736-740. [doi:10.1109/OCEANS.2007.4449219]

Papastergiou, K.D., Macpherson, D.E., 2007a. An airborne radar power supply with contactless transfer of energy-Part I: rotating transformer. *IEEE Trans. Ind. Electron.*, **54**(5):2874-2884. [doi:10.1109/TIE.2007.902044]

Papastergiou, K.D., Macpherson, D.E., 2007b. An airborne radar power supply with contactless transfer of energy-Part II: converter design. *IEEE Trans. Ind. Electron.*, **54**(5):2885-2893. [doi:10.1109/TIE.2007.901370]

Papastergiou, K.D., Macpherson, D.E., 2008. Air-Gap Effects in Inductive Energy Transfer. IEEE Power Electronics Specialists Conf., **1-10**:4092-4097. [doi:10.1109/PESC.2008.4592594]

Ryu, M., Cha, H., Park, Y., Baek, J., 2005. Analysis of the Contactless Power Transfer System Using Modelling and Analysis of the Contactless Transformer. 31st Annual Conf. of the IEEE Industrial Electronics Society, **1-3**:1036-1042. [doi:10.1109/IECON.2005.1569047]

Si, P., Hu, A.P., Malpas, S., Budgett, D., 2008. A frequency control method for regulating wireless power to implantable devices. *IEEE Trans. Biomed. Circ. Syst.*, **2**(1):22-29. [doi:10.1109/TBCAS.2008.918284]

Stielau, O.H., Covic, G.A., 2000. Design of Loosely Coupled Inductive Power Transfer Systems. Proc. Int. Conf. on Power System Technology, p.85-90. [doi:10.1109/ICPST.2000.900036]

Villa, J.L., Sallan, J., Llombart, A., Sanz, J.F., 2009. Design of a high frequency inductively coupled power transfer system for electric vehicle battery charge. *Appl. Energy*, **86**(3):355-363. [doi:10.1016/j.apenergy.2008.05.009]

Wang, C.S., Covic, G.A., Stielau, O.H., 2004. Power transfer capability and bifurcation phenomena of loosely coupled inductive power transfer systems. *IEEE Trans. Ind. Electron.*, **51**(1):148-157. [doi:10.1109/TIE.2003.822038]

Wang, J., Witulski, A.F., Vollin, J.L., Phelps, T.K., Cardwell, G.I., 1999. Derivation, Calculation and Measurement of Parameters for a Multi-Winding Transformer Electrical Model. 14th Annual Applied Power Electronics Conf. and Exposition, p.220-226. [doi:10.1109/APEC.1999.749513]

Yoshioka, D., Sakamoto, H., Ishihara, Y., Matstumoto, T., Timischl, F., 2007. Power feeding and data-transmission system using magnetic coupling for an ocean observation mooring buoy. *IEEE Trans. Magn.*, **43**(6):2663-2665. [doi:10.1109/TMAG.2007.893775]

Zhang, N., Wang, Z.L., Fang, X., 2008. Piezoimpedane and pressure sensors with NiZn ferrite device. *Sens. Actuat. A*, **147**(2):504-507. [doi:10.1016/j.sna.2008.06.012]